Korean J. Chem. Eng., 32(6), 1081-1093 (2015)
DOI: 10.1007/s11814-014-0296-8

pISSN: 0256-1115
eISSN: 1975-7220

Evaluation of biomass component effect on kinetic values for biomass pyrolysis using simplex lattice design

Sasiporn Chayaporn*, Panusit Sungsuk*, Sasithorn Sunphorka*, Prapan Kuchonthara*,, Pornpote Piumsomboon*,**, and Benjapon Chalermsinsuwan*,**,†**

*Fuels Research Center, Department of Chemical Technology, Faculty of Science, Chulalongkorn University, 254 Phayathai Road, Patumwan, Bangkok 10330, Thailand
**Center of Excellence on Petrochemical and Material Technology, Chulalongkorn University, 254 Phayathai Road, Patumwan, Bangkok 10330, Thailand
(*Received 7 June 2014 • accepted 2 October 2014*)

Abstract−We evaluated the correlation between the biomass constituents and their kinetic values. To simplify the models and indicate the effect of each constituent, pure biomass components and their mixtures were used as biomass model. The experiments were set up based on simplex-lattice design. The pyrolysis of synthesized biomass was performed by non-isothermal thermogravimetric analyzer. Several kinetic models in the literature, including Kissinger-Akahira-Sunose, Ozawa-Flynn-Wall and analytical method were used to determine kinetic values for each experiment. The generated regression models and predicted kinetic values from those methods were compared. The results obtained from analytical model (for $n \neq 1$) showed a good agreement ($R^2 > 0.95$) with those obtained from experiments. This study also provide contour plots for all cases in order to observe the behavior of biomass pyrolysis at different component ratio.

Keywords: Simplex-lattice Design, Biomass, Pyrolysis, Model, Kinetics

INTRODUCTION

Biomass is an interesting resource that can potentially replace fossil fuel since it can be used in short cycle. It has the potential to contribute to the future energy and it is suitable for agricultural countries. Thermal decomposition such as pyrolysis, combustion and gasification is a conversion process for transformation of biomass into biofuel [1]. Pyrolysis is the well-known process for biomass conversion to energy under an absence of oxygen. It is the initial step of all thermochemical conversion processes [2,3]. In addition, pyrolysis is the simplest and easiest to set up compared to gasification [4,5].

The kinetics of biomass decomposition is the key to understanding the mechanism and designing a suitable conversion process. Non-isothermal thermogravimetric analysis (TGA) is one of the best methods for the study of the kinetics of pyrolysis. Several kinetic methods were used to calculate kinetic parameters including the activation energy, frequency factor and reaction order from TGA data with various factor effects [3,6-12]. Among several kinetic models, the iso-conversional methods such as The Kissinger - Akahira - Sunose (KAS) method and Ozawa-Flynn-Wall (OFW) method are the most commonly accepted for computational calculation based on TGA and successfully used to simulate the pyrolysis behavior of biomass [3,13-15]. These kinetic models were developed from single-step pyrolysis. They calculate the kinetic parameters with a progress of conversion and temperature without considering the reaction mechanism [16]. The previous literature study reported that KAS and OFW methods are reliable enough for calculating activation energy of cardoon pyrolysis from TGA data [3]. Besides these two kinetic models, the analytical model, which is derived from single-step decomposition kinetics, was also selected [7,10,11]. The analytical model derived by an assumption of n^{th}-order kinetics is reported to be acquirable, representative, and reliable for biomass pyrolysis [7]. The calculated kinetic values obtained from all models revealed that pyrolysis of biomass were complex and multi-step kinetics.

To simplify the calculation of kinetic parameters, the prediction of kinetic parameters from biomass composition has been explored [17-21]. The correlations between main biomass components and each kinetic parameter were proposed instead of a calculation from TGA data. The previous study described the thermal degradation of pistachio shells by a detailed reaction mechanism [20]. The results indicated that the expected mass loss during pistachio shell pyrolysis derived from reaction mechanisms and discrete particle method agreed well with experimental data. However, the major advantage of the developed model is that it could employ the pyrolysis mechanism, but the model is very complex. Moreover, some studies detected the differences between predicted values and experimental data which were probably due to the interactions between compounds and extractives [19,21]. Therefore, the development of simply and accurate models which can potentially predict the thermal behavior and kinetic values is still attractive.

Besides the development of models from reaction mechanisms, many studies attempted to use the mathematical and statistical meth-

†To whom correspondence should be addressed.
E-mail: benjapon.c@chula.ac.th

ods for finding the correlation between biomass main components and kinetic parameters. Response surface methodology (RSM), based on simplex-lattice design, was chosen and demonstrated as a suitable method for examining the effect of correlated three input components on the output data [22,23]. It is suitable for investigating the biomass system since biomass' three main components and summation of three proportions might be assumed to one. The previous study used simplex-lattice design (SLD) to determine the interaction between the biomass components during synthesized biomass pyrolysis [23]. The effect of each component and its interactions on mass loss rate could be observed. However, this study did not provide the other kinetic values.

However, there is a lack of applying this kind of model to this research field. Therefore, the aim of this study was to develop a simplified model for predicting kinetic values for biomass pyrolysis from its main components. The correlations between mass fractions of cellulose, hemicellulose and lignin were the input data, while output data were activation energy, pre-exponential factor and reaction order. The RSM based on SLD was chosen as a tool for this purpose. For each point of experimental design, the synthesized biomass was prepared at the desired ratio. The kinetic values were evaluated from TGA data using the isoconversional methods, including KAS and OFW methods, and also analytical method (in cases of first-order kinetics and n^{th}-order kinetics). The calculated kinetic parameters obtained from three kinetic models (six cases) were compared. The statistical analyses were also provided for all six cases. The effect of pure biomass components and their interactions were identified for each case and discussed. The regression models and contour plots for predicted kinetic parameters were also provided in this study to observe the interactions of biomass components.

MATERIALS AND METHODS

1. Materials

Pure a-cellulose, xylan (a model of hemicellulose), and organosolv lignin were purchased from Sigma Aldrich. The real biomass, *Leucaena Leucocephala*, was used to check the accuracy of the model. The lignin content was analyzed by Tappi T222om-98 [24]. The holocellulose content (cellulose and hemicellulose) was analyzed by the Browning method of wood chemistry [25], whilst the a-cellulose content was analyzed by Tappi T203om-88 [26]. The *Leucaena Leucocephala* was ground by biomass grinder and filtered into particle sizes of 150-250 micron. The synthesized biomass and real biomass were dried at 110 °C for 24 h before use.

2. Experimental Design

The simplex-lattice design (SLD) was used to determine the number of experiments and evaluate the effect of mass fraction of cellulose (X_1), mass fraction of hemicellulose (X_2) and mass fraction of lignin (X_3) on kinetic parameters including activation energy (E_a), frequency factor (A) and reaction order (n). The samples were prepared by physical mixing of the three pure components at different ratios. Based on SLD, summation of mass fractions ($X_1+X_2+X_3$) is unity. The sample codes for total 13 combinations and the mass fraction of each experimental design point are presented in Table 1. The 13 experimental points were three single-component treatments (Nos. 1, 2 and 3), six two-component mixtures (Nos. 4, 5, 8, 10, 11 and 13) and four three-component mixtures (Nos. 6, 7, 9 and 12). For each mixture, the experiments were performed at four linear heating rates (5, 10, 20 and 40 °C min^{-1}) with replicates.

Table 1. Sample code and mass fractions of cellulose, hemicellulose and lignin

Sample code	Mass fraction		
	Cellulose	Hemicellulose	Lignin
1	1.00	0.00	0.00
2	0.00	1.00	0.00
3	0.00	0.00	1.00
4	0.00	0.33	0.67
5	0.00	0.67	0.33
6	0.17	0.17	0.67
7	0.17	0.67	0.17
8	0.33	0.00	0.67
9	0.33	0.33	0.33
10	0.33	0.67	0.00
11	0.67	0.00	0.33
12	0.67	0.17	0.17
13	0.67	0.33	0.00

3. Thermogravimetric Analysis (TGA)

At each experimental run based on SLD, the weight loss and differential weight loss of synthesized and real biomass pyrolysis were observed by thermogravimetric/differential thermal analyzer (Mettler Toledo TG Analyzer) under nitrogen atmosphere. The flow rate of nitrogen gas was 50 mL min^{-1}. Approximately 3.0 mg of sample was placed into an aluminum pan. The sample was heated from 30 to 1,000 °C at four linear heating rates.

4. Kinetic Models

The values of kinetic parameters were calculated by data interpretation of thermogravimetric analysis (TGA) and differential thermal analysis (DTA) curves, since they present the overall weight loss rate of biomass pyrolysis. The biomass pyrolysis can be described by three kinetic models, including Kissinger-Akahira-Sunose (KAS), Ozawa-Flynn-Wall (OFW) and analytical model. These methods are based on the assumptions that the reaction rate at constant extent of conversion is only a function of temperature [27], and they take into consideration the one-step process decomposition [3]. This study's apparent kinetic ignores the effect of particle size (heat and mass transfers) since the real pyrolysis process might be operated by using different particle sizes of biomass.

The general reaction rate is expressed as

$$\frac{d\alpha}{dt} = k(T)f(\alpha) \quad (1)$$

where α is the conversion of convertible part of biomass and calculated from $\alpha=(W_o-W)/(W_o-W_{ash})$; W_0 is the original weight, W is the weight at any time t and W_{ash} is the ash content in the sample. The function k(T) is the rate constant given by Arrhenius equation, while the function $f(\alpha)$ depends on the decomposition mechanism.

By combining the constant heating rate (β=dT/dt) and Arrhe-

nius equation, Eq. (1) can be shown as Eq. (2).

$$\frac{d\alpha}{f(\alpha)} = \frac{A}{\beta}\exp\left(-\frac{E_a}{RT}\right)dT \quad (2)$$

Gives:

$$g(\alpha) = \int_0^{\alpha}\frac{d\alpha}{f(\alpha)} = \int_0^{\alpha}\frac{A}{\beta}\exp\left(-\frac{E_a}{RT}\right)dT = \frac{AE_a}{\beta R}p\left(\frac{E_a}{RT}\right) \quad (3)$$

where E_a is the activation energy (kJ/kmol), R is a gas constant (8.314 kJ/kmol·K) and T is the reaction temperature (K). The term $p(E_a/RT)$ is the temperature integral. The difference of iso-conventional methods is due to the approximation for solving the equation.

4-1. Kissinger-Akahira-Sunose Model (KAS) [27-29]

The approximation is proposed to be:

$$p\left(\frac{E_a}{RT}\right) = \exp\left(-\frac{E_a}{RT}\right)\times\left(\frac{E_a}{RT}\right)^{-2} \quad (4)$$

Substitutes Eq. (4) into Eq. (3) and takes logarithm. Then, Eq. (3) becomes:

$$\ln\left(\frac{\beta}{T^2}\right) = \ln\left(\frac{AE_a}{Rg(\alpha)}\right) - \frac{E_a}{RT} \quad (5)$$

E_a and A can be calculated by plotting curve of $\ln(\beta/T^2)$ versus 1/T. In this study, the $g(\alpha)$ is equal to $-\ln(1-\alpha)$ for first-order kinetics and $(n-1)^{-1}(1-\alpha)^{(1-n)}$ for any order n.

4-2. Ozawa-Flynn-Wall (OFW) [27,30,31]

The approximation of this model is based on Doyle's approximation [32]. Therefore, Eq. (3) becomes:

$$\log\beta = \log\left(A\frac{E_a}{Rg(\alpha)}\right) - 2.315 - 0.457\left(\frac{E_a}{RT}\right) \quad (6)$$

E_a and A can be calculated by plotting curve of $\log(\beta)$ versus 1/T. The function $g(\alpha)$ is the same as indicating in Section 2.4.1.

4-3. Analytical Model

This model is derived based on single step decomposition process. Therefore, the function $f(\alpha)$ in Eq. (2) is equal to $(1-\alpha)^n$. Then, Eq. (2) becomes:

$$\frac{d\alpha}{dT} = \frac{A}{\beta}\exp\left(-\frac{E_a}{RT}\right)(1-\alpha)^n \quad (7)$$

After solving the equation, the equations for analytical method are given below:

for first-order kinetics:

$$\alpha = 1-\exp\left\{-\frac{ART^2}{\beta E_a}\left(1-\frac{2RT}{E_a}\right)\exp\left(-\frac{E_a}{RT}\right)\right\} \quad (8)$$

for n^{th}-order kinetics:

$$\alpha = 1-\left\{1-(n-1)\left(-\frac{ART^2}{\beta E_a}\right)\left(1-\frac{2RT}{E_a}\right)\exp\left(-\frac{E_a}{RT}\right)\right\}^{\frac{1}{1-n}} \quad (9)$$

To calculate the kinetic parameters including E_a and A, the TGA curves were fitted with analytical models (Eqs. (8) and (9)) by means of maximizing the regression coefficient (R^2). In case of any order n of all methods, n was calculated by Kissinger index of shape equation. The shape index is defined as the absolute value of the ratio of the slope of tangents to the curve at inflection points of differential thermal analysis (DTA) curves [28,33].

The pyrolysis of real example biomass, *Leucaena Leucocephala*, was also performed. The kinetic parameters were calculated from the proposed models. Then, the conversion curves obtained from kinetic values of different methods were compared to that obtained from experiment.

5. Statistical Analysis and Modeling

An analysis of variance (ANOVA) and response surface methodology (RSM) were used to evaluate the effect of each biomass constituent, determine the most significant factor on the desired response and also generate the statistical models for predicting the kinetic parameters. The model is expressed in terms of cubic equation (Eq. (10)) [22,34].

$$Y = a_1X_1 + a_2X_2 + a_3X_3 + a_{12}X_1X_2 + a_{13}X_1X_3 + a_{23}X_2X_3 + a_{1-2}X_1X_2(X_1-X_2) + a_{1-3}X_1X_3(X_1-X_3) + a_{2-3}X_2X_3(X_2-X_3) \quad (10)$$

where Y is an estimated response (E_a, A or n). The a_1, a_2, a_3, a_{12}, a_{13}, a_{23}, a_{1-2}, a_{1-3} and a_{2-3} are constant coefficients for linear and nonlinear (interaction) terms. The direction and magnitude of coefficients can illustrate the effect of each term on the desired response. The models were also used to generate the ternary contour plots in order to observe the influence of biomass compositions on E_a, A and n. The models and ternary contour plots for estimated kinetic values obtained from different kinetic models were produced and compared to each other.

RESULTS AND DISCUSSION

1. Evaluation of Kinetic Values from Different Kinetic Models

Table 2 presents the E_a and A calculated from different kinetic models based on first-order kinetics. The results were averaged from eight replicates (four heating rates with two replicates per each). Both values calculated from KAS and OFW have the same trend and comparable values, because both methods are developed from the same assumption with different approximations of $p(E_a/RT)$. The results obtained from both methods indicated that pure lignin gave the highest E_a (~200 kJ/mol), while pure hemicellulose and hemicellulose: lignin mixture at 0.33 : 0.67 wt : wt gave the lowest E_a (~120-130 kJ/mol). However, in case of mixtures, a different trend was observed. Mixtures with high cellulose and hemicellulose proportion gave higher E_a compared to those with high lignin proportion. Moreover, the values of E_a and *A* in cases of mixtures cannot be calculated from the arithmetic method (e.g., summation of mass fractions multiplied by E_a and *A* of pure components). It might be due to the interaction between each component.

Considering the case of analytical method, some differences occurred. The calculated E_a and *A* values were much lower than those obtained from KAS and OFW methods in many cases. The large differences were probably because the analytical method attempts to fit the model with experimental data without considering the pyrolysis behavior, while the isoconversional method approximates the reaction order from DTA data and calculates other kinetic values from larger information (simultaneously calculated from different heating rates and progress of conversion). Anyway, the accuracy of models was tested and is discussed further down.

Table 2. Predicted kinetic values obtained from different decomposition models

Sample code	KAS		OFW		Analytical method	
	E_a (kJ/mol)	A (min^{-1})	E_a (kJ/mol)	A (min^{-1})	E_a (kJ/mol)	A (min^{-1})
1	145.0	1.0E+12	147.6	2.0E+12	143.2	3.7E+12
2	123.0	9.7E+10	126.0	2.2E+11	90.0	1.8E+06
3	199.8	2.3E+16	199.9	2.4E+16	103.4	4.4E+05
4	120.8	4.0E+10	124.0	8.2E+10	103.9	2.8E+06
5	164.5	2.7E+14	165.5	7.1E+10	69.3	6.7E+05
6	142.0	2.6E+11	145.0	5.3E+11	104.8	1.7E+06
7	165.8	8.8E+14	166.6	1.2E+15	95.5	1.8E+06
8	179.9	1.0E+15	181.0	1.2E+15	108.2	1.6E+07
9	141.2	1.8E+11	144.3	3.7E+11	103.9	2.1E+06
10	164.4	6.2E+14	165.3	8.0E+14	104.5	1.8E+07
11	142.0	2.6E+11	134.9	4.9E+11	93.9	2.5E+07
12	169.7	3.5E+15	171.5	3.9E+15	86.1	6.0E+04
13	183.6	6.3E+13	184.7	2.5E+15	90.7	6.4E+05
Biomass	178.6	1.0E+15	179.5	1.3E+15	100.4	1.7E+06

The highest E_a and A values, in this case, were obtained from a case of pure cellulose while the lowest E_a was obtained from a case of hemicellulose: lignin mixture at 0.67 : 0.33 wt : wt (Sample no. 5). In addition, the mixtures with high cellulose proportion gave lower E_a, while the mixtures with higher lignin proportion gave higher E_a, excepting sample 5. This phenomenon was also reported in the literature [21]. The previous study demonstrated that higher E_a is required to decompose woody biomass, which has higher lignin content. It is because the complex aromatic structure of lignin. The interactions were also observed in this case. The differences of results obtained from the former methods and those obtained from analytical method were probably due to different assumptions of reaction mechanism in forms of function $f(\alpha)$ as mentioned in Section 2.4.

Table 3 provides the values of E_a, A and n calculated from different kinetic models based on n^{th}-order kinetics. The results were also averaged from eight replicates. It should be noted that the E_a calculated from cases of first-order (Table 2) and n^{th}-order kinetics (Table 3) for both KAS and OFW had the same values, because they were calculated from the slope of linear plots which do not involve the calculation of n. The A and n were calculated from the intercept of linear plots. However, even though the calculated A obtained from cases of first-order and n^{th}-order kinetics were different, the trend was still the same.

Considering the calculated n, Table 3 shows that the apparent reaction orders of biomass pyrolysis are larger than one, especially in the case of using the analytical method. KAS and OFW gave the same n values since they were calculated from the same DTA curve. It can be seen that reaction order obtained from pure components was lower than those obtained from mixtures. When the different compound was added to other compounds, the several decomposition reactions were parallel occurring due to the decom-

Table 3. Predicted kinetic values obtained from different decomposition models for n≠1

Sample code	KAS			OFW			Analytical method		
	E_a (kJ/mol)	A (min^{-1})	n (-)	E_a (kJ/mol)	A (min^{-1})	n (-)	E_a (kJ/mol)	A (min^{-1})	n (-)
1	145.0	1.50E+12	1.4	147.6	2.80E+12	1.4	178.1	9.38E+13	1.6
2	123.0	1.60E+11	1.5	126.0	5.00E+12	1.5	83.6	7.60E+07	1.1
3	199.8	2.50E+16	1.2	199.9	2.20E+12	1.2	68.3	1.82E+05	1.1
4	120.8	5.00E+10	1.3	124.0	1.20E+11	1.3	74.3	4.00E+04	6.2
5	164.5	4.80E+14	1.6	165.5	7.80E+14	1.6	72	1.10E+05	6.5
6	142.0	5.20E+11	1.8	145.0	1.10E+12	1.8	74.5	3.60E+04	5.9
7	165.8	1.40E+15	1.5	166.6	3.50E+12	1.5	82.1	3.80E+07	6.4
8	179.9	1.70E+15	1.6	181.0	2.10E+15	1.6	117.6	6.40E+08	7.1
9	141.2	3.10E+11	1.6	144.3	4.90E+12	1.6	89	2.10E+06	6.5
10	164.4	1.20E+15	1.6	165.3	1.50E+15	1.6	84.7	6.80E+07	5.8
11	142.0	3.90E+11	1.5	134.9	8.60E+11	1.5	127.6	1.10E+09	5.9
12	169.7	5.20E+15	1.5	171.5	3.10E+12	1.5	118.9	6.40E+08	5.6
13	183.6	4.40E+15	1.7	184.7	5.10E+15	1.7	81.3	9.80E+05	4.8
Biomass	178.6	3.10E+15	2	179.5	3.80E+15	2	125.1	9.70E+09	1.4

position of the added compounds and also interactions between all components. Multiple reactions including several parallel first-order reactions can be expressed by an apparent n^{th}-order reaction [35]. The calculated n was thus increased in case of mixture.

In case of using analytical method, n values for pyrolysis of the mixtures were much higher than those obtained from KAS and OFW. Higher lignin content gave higher n values. Besides the n, the trends of E_a and A were different from those obtained from other isoconversional methods. The highest E_a was obtained in a case of pure cellulose, higher than a case of pure lignin. Higher cellulose content needed higher E_a during pyrolysis based on these results.

Besides the pyrolysis of synthesized biomass, real biomass pyrolysis, *Leucaena Leucocephala*, was performed. The kinetic values of biomass pyrolysis are presented in Tables 2 and 3 as well. The n obtained from this method was very large compared to that obtained from other models, indicating very complex reactions occurred. Fig. 1(a) and (b) show the conversion curves obtained from calculated kinetic values. Fig. 1(a) presents the conversion curves for case of first-order kinetics, and Fig. 1(b) presents the curves for n^{th}-order kinetics. The regression coefficients (R^2) for each case are shown in Table 4. The conversion rate of Fig. 1(a) and 1(b) was calculated by Eq. (1) with the initial and final temperatures of 100 °C and 700 °C, respectively. This temperature range ignores the weight change due to the evaporation of moisture and focuses mainly on the decomposition or pyrolysis step of biomass. The pyrolysis of biomass commonly occurs in this temperature range [3,8,10,11,37]. Conversion curves obtained from the analytical model showed the best fit to experimental data, possibly because the analytical method was fitted to experimental data directly to calculate the kinetic parameters, resulting in the highest R^2. However, differences were observed between experimental and predicted data at relatively low temperature and high temperature. It was due to the assumption of the kinetic model since the kinetic model was developed based on single-step decomposition. In fact, the biomass pyrolysis involves multi-step degradation. At low temperature, the conversion is due to the moisture evaporation, while the conversion at high temperature is due to lignin degradation. Therefore, the deviation of predicted values from experimental values was sometimes observed at these steps. However, the predicted conversion rate was highly accurate at the session in which mostly decomposition occurred.

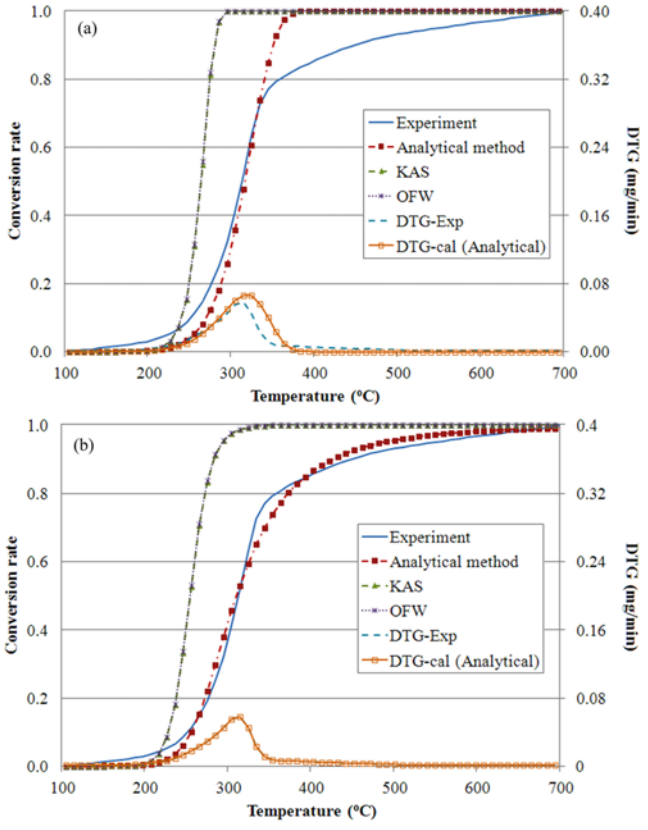

Fig. 1. Relation between temperature and conversion (wt/wt) of biomass pyrolysis obtained from different methods for first-order kinetics (a) and any-order kinetics (b).

Table 4. Regression coefficients of the decomposition curves generated from KAS, OFW and analytical method for biomass pyrolysis

Method	Regression coefficients (R^2)	
	n=1	n≠1
KAS	0.77	0.73
OFW	0.76	0.73
Analytical method	0.98	1.00

In case of isoconversional methods, they also simulate the biomass pyrolysis as a one-step process and neglect the physical and chemical nature of the pyrolysis process. The details in diffusion, adsorption, desorption and other occurring phenomena as well as the whole reaction scheme are not considered [3]. The errors in the calculated values obtained from KAS and OFW were probably due to the assumption of f(a) and g(α). The other reaction models including nucleation or diffusional model might be applied instead.

2. Statistical Analysis and Modeling

2-1. Analysis of Variance for First-order Kinetics

To evaluate the effect of cellulose, hemicellulose and lignin on the kinetic parameters and understand the interaction between them, the simplex-lattice design was used. Based on this experimental design, the synthesized biomass was prepared as described in Section 2.2. Then ANOVA was applied to analyze the effect of response as described in Section 2.5. The *p*-value indicates the probability of kinetic parameters affected from each term of model. The terms which have *p*-value less than 0.05 have an important effect on the kinetic parameters during biomass pyrolysis. All analysis results are shown in Appendix A (Table A.1). For the case of using the KAS model, the results demonstrated that the interaction terms including quadratic term between cellulose and hemicellulose (X_1X_2) and cubic term between hemicellulose and lignin ($X_2X_3(X_2-X_3)$) had a statistically significant effect on E_a. By the same way, the results indicated that the linear terms, interaction terms including X_1X_3, X_2X_3, $X_1X_3(X_1-X_3)$ and $X_2X_3(X_2-X_3)$, had a statistically significant effect on *A*. In case of using OFW, the important factors which have significant effect on both parameters were almost the same as the case of using KAS, excepting the $X_1X_2X_3$ term. As mentioned above, both KAS and OFW were developed by the same way excepting

an approximation of g(α). Therefore, the calculated kinetic values and also ANOVA for both cases were comparable.

For the analytical method, the analysis results were different. The statistical analysis results presented that the linear terms and interaction including X_1X_3 and $X_1X_2(X_1-X_2)$ had a significant effect on E_a while all terms excluding X_2X_3 and $X_2X_3(X_2-X_3)$ had significant effect on A. The effect of each component was unclear in case of E_a. However, in case of A, it seems that the cellulose proportion was the dominant factor since all terms containing X_1 had a significant effect on A. This result differs from other models. Considering the trend of conversion curves in Fig. 1 and R^2 values in Table 4, the calculated kinetic parameters obtained from analytical method provided higher R^2. Therefore, the analysis results obtained from this model must be concerned. The cellulose pyrolysis has higher decomposition rate due to its simple ordered repeating unit, cellobiose. The TGA data (not shown here) indicated that cellulose decomposes rapidly in a narrow temperature range, resulting in high reaction rate, while lignin decomposes at wider temperature range. This observation was consistent with other previous studies [36,37]. The cellulose pyrolysis thus influenced the decomposition rate for all synthesized biomass which contain cellulose in their composition.

2-2. Analysis of Variance for n^{th}-order Kinetics

The statistical analysis results are shown in Appendix A (Table A.2). In this section, only the analysis results for case of using analytical method (Table A.2(g)-(i)) are discussed. The results indicated that linear terms and interaction between cellulose and hemicellulose (X_1X_2) had a significant effect on E_a. No interaction effect was observed. In case of A, the effluent factors were the same as the case of first-order kinetics, which confirmed that cellulose acts as the dominant factor on decomposition rate of biomass pyrolysis. For n, the two quadratic terms and interactions between all pure components ($X_1X_2X_3$) were indicated as the important factors. The interactions between all pure components were obviously seen since the n values of pure components were below two (Table 3) and dramatically increased by mixing together. The several components contain in hemicellulose and lignin provided parallel n^{th}-order reaction, leading to higher n.

The ANOVA analysis for KAS and OFW methods is also provided in Table A.2. As expected, the results for E_a and n obtained from both methods are similar. However, the case of *A* was different. It is difficult to determine what makes the large difference on statistical analysis between these methods. Table 3 shows that the calculated values of A were almost equal and comparable. In addition, the only one thing which is different from each other is the approximation of g(α) term.

2-3. Modeling and Ternary Contour Plot

To predict and observe the variation of E_a, A and n at different biomass compositions, the regression models and contour plots were also generated. The regression models for predicting kinetic parameters based on analytical method are shown in Appendix B (Eqs. (B.1)-(B.5)). Considering the coefficient of each term, it provided an insight into ranking the importance of each term correspondence with the ANOVA analysis. The positive coefficient indicated that an increase in term magnitude increased the kinetic values, while the negative coefficient indicated the opposite effect. The R^2 values of all models were above 0.95, which revealed very good agreement of predicted values from regression models and experiments.

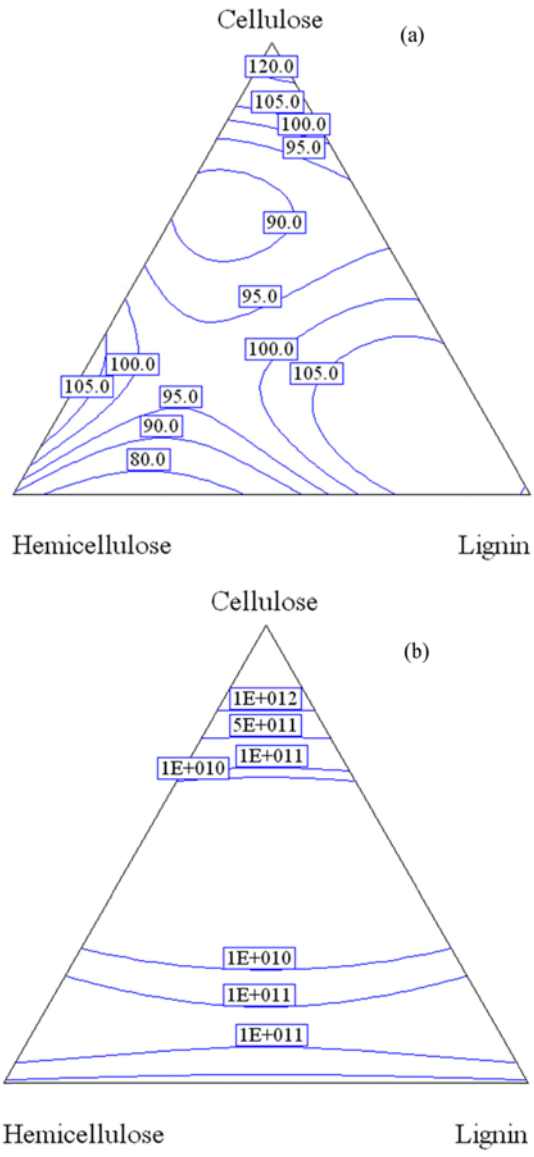

Fig. 2. Ternary contour plots of predicted activation energy (a) and pre-exponential factor (b) obtained from analytical method for first-order kinetics.

The response of each kinetic parameter was graphically represented as ternary contour plot (Figs. 2 and 3). Based on SLD, all 13 points of experiments are located inside the triangle. It means that the sum of proportions of cellulose, hemicellulose and lignin was always unity. Fig. 2 shows the contour plots of E_a and A for first-order kinetics and Fig. 3 shows the plots for n^{th}-order kinetics, with respect to the regression models. The interactions between biomass components were obviously seen. The variation in biomass composition was the important key to predict the kinetic of its pyrolysis and observe the thermal behavior as well.

Regression models and ternary contour plots for predicting kinetic parameters based on KAS and OFW methods were also provided in Appendices B and C, respectively. All regression models, exclud-

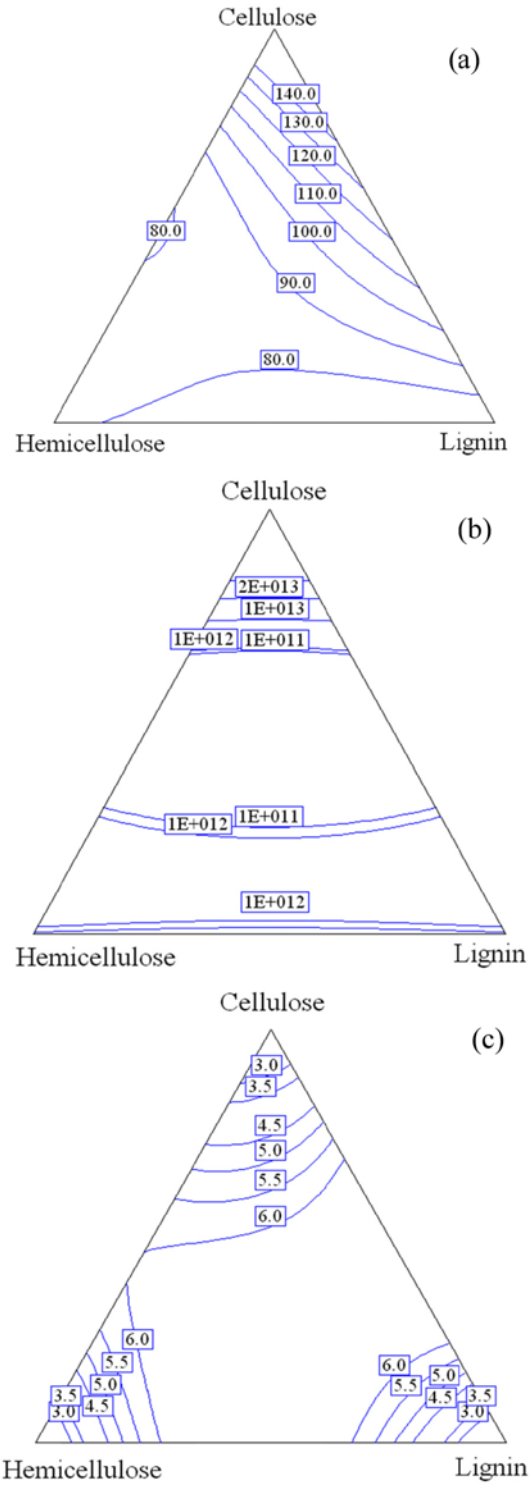

Fig. 3. Ternary contour plots of predicted activation energy (a), pre-exponential factor (b) and reaction order (c) obtained from analytical method for n^{th}-order kinetics.

ing the case of n, had high R^2. The relatively low R^2 of regression model for n revealed that the model could not be used to predict the accurate values for those kinetic models. On the other hand, the model generated from SLD might not do enough to predict the values of n obtained from Kissinger index of shape equation.

CONCLUSIONS

The variation of biomass composition plays an important role in its thermal behavior. The calculated kinetic values from three kinetic models showed the different results and trend. Compared to the conversion curve of real biomass, the conversion curve generated from analytical method showed the best fit compared to that obtained from other kinetic models. Based on SLD and analytical model, cellulose proportion was the most important factor influencing the A and n. The proposed regression models showed very high R^2 values, almost equal to unity. The generated contour plots could be used to observe the variation of kinetic parameters at different biomass composition.

ACKNOWLEDGEMENT

This study was financially supported by grants from the Thailand Research Fund for fiscal year 2014-2016 (TRG5780205), the grant for Development of New Faculty Staff (Ratchadaphisek Somphot Endowment Fund) of Chulalongkorn University, the grant from Faculty of Science of Chulalongkorn University and the Center of Excellence on Petrochemical and Materials Technology, Chulalongkorn University. In addition, the authors would like to express their thanks to the Graduate School, Chulalongkorn University for partial financial support.

REFERENCES

1. N. Choobuathong, *Effects of chemical composition of biomass on pyrolysis and combustion*, Department of Chemical Technology, Chulalongkorn University, Bangkok (2007).
2. J. Jones, *Chem. Eng.*, **85**, 87 (1978).
3. T. Damartzis, D. Vamvuka, S. Sfakiotakis and A. Zabaniotou, *Bioresour. Technol.*, **102**, 6230 (2011).
4. J. M. Encinar, J. F. Gonzalez and J. Gonzalez, *Fuel Process. Technol.*, **68**, 209 (2000).
5. E. Mura, O. Debono, A. Villot and F. Paviet, *Biomass Bioenergy*, **59**, 187 (2013).
6. Y. F. Huang, P. T. Chiueh, W. H. Kuan and S. L. Lo, *Appl. Energy*, **110**, 1 (2013).
7. Y. F. Huang, W. H. Kuan, P. T. Chiueh and S. L. Lo, *Bioresour. Technol.*, **102**, 9241 (2011).
8. S. Hu, A. Jess and M. Xu, *Fuel*, **86**, 2778 (2007).
9. A. Meng, H. Zhou, L. Qin, Y. Zhang and Q. Li, *J. Anal. Appl. Pyrol.*, **104**, 28 (2013).
10. S. Ren, H. Lei, L. Wang, Q. Bu, S. Chen and J. Wu, *Biosystems Eng.*, **116**, 420 (2013).
11. S. Singh, C. Wu and P. T. Williams, *J. Anal. Appl. Pyrol.*, **94**, 99 (2012).
12. J. Chattopadhyay, C. Kim, R. Kim and D. Pak, *Korean J. Chem. Eng.*, **25**, 1047 (2008).
13. S. Unz, T. Wen and M. Beckmann, *Characterization of biomass used in thermal processes with regard to the kinetic properties*, 35th International Technical Conference on Clean Coal & Fuel Systems, Clearwater, Florida, USA (2010).
14. C. Chen, X. Ma and Y. He, *Bioresour. Technol.*, **117**, 264 (2012).

15. S. Ceylan and Y. Topçu, *Bioresour. Technol.*, **156**, 182 (2014).
16. A. Khawam, *Application of solid-state kinetics to desolvation reactions*, Pharmacy, Graduate College of The University of Iowa, Iowa, USA (2007).
17. A. Garcia-Maraver, D. Salvachua, M. J. Martinez, L. F. Diaz and M. Zamorano, *Waste Manage.*, **33**, 2245 (2013).
18. A. Gani and I. Naruse, *Renew. Energy*, **32**, 649 (2007).
19. C. Couhert, J.-M. Commandre and S. Salvador, *Fuel*, **88**, 408 (2009).
20. B. Peters, *Fuel Process. Technol.*, **92**, 1993 (2011).
21. L. Burhenne, J. Messmer, T. Aicher and M.-P. Laborie, *J. Anal. Appl. Pyrol.*, **101**, 177 (2013).
22. P. V. Rao and S. S. Baral, *Chem. Eng. J.*, **172**, 977 (2011).
23. Q. Liu, Z. Zhong, S. Wang and Z. Luo, *J. Anal. Appl. Pyrol.*, **90**, 213 (2011).
24. TAPPI PRESS, Atlanta, USA. TAPPI Standard T-222 om-98, "Acid-insoluble lignin in wood and pulp, TAPPI Test Methods", TAPPI PRESS, Atlanta, USA (1998).
25. B. L. Browning, *Methods of wood chemistry*, Wiley Inter-Science Publishers, New York (1967).
26. TAPPI Official Test Method T 203 om-88, "Alpha-, Beta-, and Gamma-Cellulose in Pulp", the TAPPI Press, Atlanta, Georgia, revised 1988, correction 1992, pp. 1-3 (1988).
27. J. E. White, W. J. Catallo and B. L. Legendre, *J. Anal. Appl. Pyrol.*, **91**, 1 (2011).
28. H. E. Kissinger, *Anal. Chem.*, **29**, 1702 (1957).
29. T. Akahira and T. Sunose, *Research Report of Chiba Institute of Technology*, **16**, 22 (1971).
30. T. Ozawa, *J. Therm. Anal.*, **2**, 301 (1970).
31. J. H. Flynn, *Thermochim. Acta*, **300**, 83 (1997).
32. C. D. Doyle, *Nature*, **207**, 290 (1965).
33. C.-P. Lin, Y.-M. Chang, J. P. Gupta and C.-M. Shu, *Process. Safe. Environ.*, **88**, 413 (2010).
34. S. Karaman, M. T. Yilmaz and A. Kayacier, *Food Hydrocolloid.*, **25**, 1319 (2011).
35. K. Hashimoto, I. Hasegawa, J. Hayashi and K. Mae, *Fuel*, **90**, 104 (2011).
36. H. Zhou, Y. Long, A. Meng, Q. Li and Y. Zhang, *Thermochim. Acta*, **566**, 36 (2013).
37. H. Haykiri-Acma, S. Yaman and S. Kucukbayrak, *Fuel Process. Technol.*, **91**, 759 (2010).

APPENDIX A

ANOVA analysis of kinetic parameters from KAS, OFW and analytical method (first-order kinetics)

Table A.1. The analysis of variance (ANOVA) for first-order kinetic values of biomass pyrolysis

(a) Activation energy obtained from KAS method

Source	Sum of squares	DF	Mean square	F value	*P*-value>F
Model	6,494.30	9	721.59	9.22	0.05
Linear mixture	618.21	2	309.10	3.95	0.14
X_1X_2	1,716.32	1	1,716.32	21.93	0.02[a]

Table A.1. Continued

(a) Activation energy obtained from KAS method

Source	Sum of squares	DF	Mean square	F value	*P*-value>F
X_1X_3	116.37	1	116.37	1.49	0.31
X_2X_3	393.69	1	393.69	5.03	0.11
$X_1X_2X_3$	147.75	1	147.75	1.89	0.26
$X_1X_2(X_1-X_2)$	198.97	1	198.97	2.54	0.21
$X_1X_3(X_1-X_3)$	100.62	1	100.62	1.29	0.34
$X_2X_3(X_2-X_3)$	3,096.39	1	3,096.39	39.56	0.01[a]
Residual	234.82	3	78.27		
Total	6,729.13	12			

(b) Pre-exponential factor obtained from KAS method

Source	Sum of squares	DF	Mean]square	F value	*P*-value>F
Model	4.61E+32	9	5.12E+31	42.45	0.01[a]
Linear mixture	1.65E+32	2	8.26E+31	68.46	>0.00[a]
X_1X_2	1.98E+29	1	1.98E+29	0.16	0.71
X_1X_3	1.16E+32	1	1.16E+32	96.34	>0.00[a]
X_2X_3	1.33E+32	1	1.33E+32	110.28	>0.00[a]
$X_1X_2X_3$	1.09E+31	1	1.09E+31	9.06	0.06
$X_1X_2(X_1-X_2)$	3.89E+29	1	3.89E+29	0.32	0.61
$X_1X_3(X_1-X_3)$	3.70E+31	1	3.70E+31	30.68	0.01[a]
$X_2X_3(X_2-X_3)$	3.63E+31	1	3.63E+31	30.07	0.01[a]
Residual	3.62E+30	3	1.21E+30		
Total	4.65E+32	12			

(c) Activation energy obtained from OFW method

Source	Sum of squares	DF	Mean square	F value	*P*-value>F
Model	6,230.46	9	692.27	6.68	0.07
Linear mixture	505.64	2	252.82	2.44	0.24
X_1X_2	1,591.80	1	1,591.80	15.35	0.03[a]
X_1X_3	225.60	1	225.60	2.18	0.24
X_2X_3	389.62	1	389.62	3.76	0.15
$X_1X_2X_3$	70.14	1	70.14	0.68	0.47
$X_1X_2(X_1-X_2)$	251.16	1	251.16	2.42	0.22
$X_1X_3(X_1-X_3)$	230.81	1	230.81	2.23	0.23
$X_2X_3(X_2-X_3)$	2,863.61	1	2,863.61	27.61	0.01[a]
Residual	311.13	3	103.71		
Total	6,541.59	12			

(d) Pre-exponential factor obtained from OFW method

Source	Sum of squares	DF	Mean square	F value	*P*-value>F
Model	5.13E+32	9	5.70E+31	112.31	>0.00[a]
Linear mixture	1.65E+32	2	8.25E+31	162.65	>0.00[a]
X_1X_2	3.16E+30	1	3.16E+30	6.23	0.09
X_1X_3	1.31E+32	1	1.31E+32	257.40	>0.00[a]
X_2X_3	1.50E+32	1	1.50E+32	295.12	>0.00[a]
$X_1X_2X_3$	8.55E+30	1	8.55E+30	16.86	0.03[a]
$X_1X_2(X_1-X_2)$	3.60E+30	1	3.60E+30	7.09	0.08
$X_1X_3(X_1-X_3)$	3.61E+31	1	3.61E+31	71.17	>0.00[a]

Table A.1. Continued

(d) Pre-exponential factor obtained from OFW method

Source	Sum of squares	DF	Mean square	F value	*P*-value>F
$X_2X_3(X_2-X_3)$	4.14E+31	1	4.14E+31	81.69	>0.00[a]
Residual	1.52E+30	3	5.07E+29		
Total	5.14E+32	12			

(e) Activation energy obtained from analytical method

Source	Sum of squares	DF	Mean square	F value	*P*-value>F
Model	3,255.28	9	361.70	7.69	0.06
Linear mixture	995.56	2	497.78	10.58	0.04[a]
X_1X_2	336.96	1	336.96	7.16	0.08
X_1X_3	559.88	1	559.88	11.90	0.04[a]
X_2X_3	107.86	1	107.86	2.29	0.23
$X_1X_2X_3$	146.81	1	146.81	3.12	0.18
$X_1X_2(X_1-X_2)$	766.25	1	766.25	16.28	0.03[a]
$X_1X_3(X_1-X_3)$	364.69	1	364.69	7.75	0.07
$X_2X_3(X_2-X_3)$	332.46	1	332.46	7.06	0.08
Residual	141.19	3	47.06		
Total	3,396.47	12			

(f) Pre-exponential factor obtained from analytical method

Source	Sum of squares	DF	Mean square	F value	*P*-value>F
Model	1.24E+25	9	1.38E+24	73.02	>0.00[a]
Linear mixture	4.68E+24	2	2.34E+24	124.38	>0.00[a]
X_1X_2	3.41E+24	1	3.41E+24	181.25	>0.00[a]
X_1X_3	3.41E+24	1	3.41E+24	181.25	>0.00[a]
X_2X_3	5.22E+20	1	5.22E+20	0.03	0.88
$X_1X_2X_3$	2.20E+23	1	2.20E+23	11.67	0.04[a]
$X_1X_2(X_1-X_2)$	7.98E+23	1	7.98E+23	42.39	0.01[a]
$X_1X_3(X_1-X_3)$	7.98E+23	1	7.98E+23	42.39	0.01[a]
$X_2X_3(X_2-X_3)$	0.00E+00	1	0.00E+00	0.00	1.00
Residual	5.65E+22	3	1.88E+22		
Total	1.24E+25	12			

[a]Significant F-values at the 95% confidence level (p-value≤0.05)
DF=Degrees of freedom

ANOVA analysis of kinetic parameters from KAS, OFW and analytical method (n^{th}-order kinetics)

Table A.2. The analysis of variance (ANOVA) for n^{th}-order kinetic values of biomass pyrolysis

(a) Activation energy obtained from KAS method

Source	Sum of squares	DF	Mean square	F value	*P*-value>F
Model	6,494.30	9	721.59	9.22	0.05
Linear mixture	618.21	2	309.10	3.95	0.14
X_1X_2	1,716.32	1	1,716.32	21.93	0.02[a]
X_1X_3	116.37	1	116.37	1.49	0.31

Table A.2. Continued

(a) Activation energy obtained from KAS method

Source	Sum of squares	DF	Mean square	F value	*P*-value>F
X_2X_3	393.69	1	393.69	5.03	0.11
$X_1X_2X_3$	147.75	1	147.75	1.89	0.26
$X_1X_2(X_1-X_2)$	198.97	1	198.97	2.54	0.21
$X_1X_3(X_1-X_3)$	100.62	1	100.62	1.29	0.34
$X_2X_3(X_2-X_3)$	3,096.39	1	3,096.39	39.56	0.01[a]
Residual	234.82	3	78.27		
Total	6,729.13	12			

(b) Pre-exponential factor obtained from KAS method

Source	Sum of squares	DF	Mean square	F value	*P*-value>F
Model	5.74E+32	9	6.38E+31	76.91	>0.00[a]
Linear mixture	1.68E+32	2	8.42E+31	101.54	>0.00[a]
X_1X_2	8.70E+30	1	8.70E+30	10.49	0.05
X_1X_3	1.41E+32	1	1.41E+32	170.22	>0.00[a]
X_2X_3	1.62E+32	1	1.62E+32	195.14	>0.00[a]
$X_1X_2X_3$	6.50E+30	1	6.50E+30	7.84	0.07
$X_1X_2(X_1-X_2)$	1.00E+31	1	1.00E+31	12.11	0.04[a]
$X_1X_3(X_1-X_3)$	3.77E+31	1	3.77E+31	45.51	0.01[a]
$X_2X_3(X_2-X_3)$	5.25E+31	1	5.25E+31	63.31	>0.00[a]
Residual	2.49E+30	3	8.29E+29		
Total	5.76E+32	12			

(c) Reaction order obtained from KAS method

Source	Sum of squares	DF	Mean square	F value	*P*-value>F
Model	0.27	9	0.03	1.23	0.48
Linear mixture	0.06	2	0.03	1.29	0.39
X_1X_2	0.03	1	0.03	1.33	0.33
X_1X_3	0.07	1	0.07	2.98	0.18
X_2X_3	0.01	1	0.01	0.34	0.60
$X_1X_2X_3$	0.00	1	0.00	0.00	0.98
$X_1X_2(X_1-X_2)$	0.01	1	0.01	0.55	0.51
$X_1X_3(X_1-X_3)$	0.08	1	0.08	3.19	0.17
$X_2X_3(X_2-X_3)$	0.00	1	0.00	0.01	0.94
Residual	0.07	3	0.02		
Total	0.34	12			

(d) Activation energy obtained from OFW method

Source	Sum of squares	DF	Mean square	F value	*P*-value>F
Model	6,230.46	9	692.27	6.68	0.07
Linear mixture	505.64	2	252.82	2.44	0.24
X_1X_2	1,591.80	1	1,591.80	15.35	0.03[a]
X_1X_3	225.60	1	225.60	2.18	0.24
X_2X_3	389.62	1	389.62	3.76	0.15
$X_1X_2X_3$	70.14	1	70.14	0.68	0.47
$X_1X_2(X_1-X_2)$	251.16	1	251.16	2.42	0.22
$X_1X_3(X_1-X_3)$	230.81	1	230.81	2.23	0.23
$X_2X_3(X_2-X_3)$	2,863.61	1	2,863.61	27.61	0.01[a]

Table A.2. Continued

(d) Activation energy obtained from OFW method

Source	Sum of squares	DF	Mean square	F value	*P*-value>F
Residual	311.13	3	103.71		
Total	6,541.59	12			

(e) Pre-exponential factor obtained from OFW method

Source	Sum of squares	DF	Mean square	F value	*P*-value>F
Model	2.48E+31	9	2.76E+30	5.46	0.09
Linear mixture	2.29E+30	2	1.14E+30	2.26	0.25
X_1X_2	1.08E+31	1	1.08E+31	21.45	0.02[a]
X_1X_3	8.52E+29	1	8.52E+29	1.69	0.28
X_2X_3	2.39E+29	1	2.39E+29	0.47	0.54
$X_1X_2X_3$	6.62E+30	1	6.62E+30	13.12	0.04[a]
$X_1X_2(X_1-X_2)$	5.09E+30	1	5.09E+30	10.07	0.05
$X_1X_3(X_1-X_3)$	4.04E+30	1	4.04E+30	8.01	0.07
$X_2X_3(X_2-X_3)$	7.02E+29	1	7.02E+29	1.39	0.32
Residual	1.51E+30	3	5.05E+29		
Total	2.63E+31	12			

(f) Reaction order obtained from OFW method

Source	Sum of squares	DF	Mean square	F value	*P*-value>F
Model	0.27	9	0.03	1.23	0.48
Linear mixture	0.06	2	0.03	1.29	0.39
X_1X_2	0.03	1	0.03	1.33	0.33
X_1X_3	0.07	1	0.07	2.98	0.18
X_2X_3	0.01	1	0.01	0.34	0.60
$X_1X_2X_3$	0.00	1	0.00	0.00	0.98
$X_1X_2(X_1-X_2)$	0.01	1	0.01	0.55	0.51
$X_1X_3(X_1-X_3)$	0.08	1	0.08	3.19	0.17
$X_2X_3(X_2-X_3)$	0.00	1	0.00	0.01	0.94
Residual	0.07	3	0.02		
Total	0.34	12			

(g) Activation energy obtained from analytical method

Source	Sum of squares	DF	Mean square	F value	*P*-value>F
Model	11,277.52	9	1253.06	8.05	0.07
Linear mixture	8,318.79	2	4159.39	26.71	0.01[a]
X_1X_2	2,109.19	1	2109.19	13.54	0.03[a]
X_1X_3	0.36	1	0.36	0.00	0.96
X_2X_3	28.79	1	28.79	0.18	0.70
$X_1X_2X_3$	12.28	1	12.28	0.08	0.80
$X_1X_2(X_1-X_2)$	421.30	1	421.30	2.71	0.20
$X_1X_3(X_1-X_3)$	58.00	1	58.00	0.37	0.58
$X_2X_3(X_2-X_3)$	0.31	1	0.31	0.00	0.97
Residual	467.23	3	155.74		
Total	11,744.76	12			

Table A.2. Continued

(h) Pre-exponential factor obtained from analytical method

Source	Sum of squares	DF	Mean square	F value	*P*-value>F
Model	8.1E+27	9	9.0E+26	73.0	>0.00[a]
Linear mixture	3.1E+27	2	1.5E+27	124.4	>0.00[a]
X_1X_2	2.2E+27	1	2.2E+27	181.3	>0.00[a]
X_1X_3	2.2E+27	1	2.2E+27	181.3	>0.00[a]
X_2X_3	3.4E+23	1	3.4E+23	0.0	0.88
$X_1X_2X_3$	1.4E+26	1	1.4E+26	11.7	0.04[a]
$X_1X_2(X_1-X_2)$	5.2E+26	1	5.2E+26	42.4	0.01[a]
$X_1X_3(X_1-X_3)$	5.2E+26	1	5.2E+26	42.4	0.01[a]
$X_2X_3(X_2-X_3)$	0.0E+00	1	0.0E+00	0.0	1.00
Residual	3.7E+25	3	1.2E+25		
Total	8.1E+27	12			

(i) Reaction order obtained from analytical method

Source	Sum of squares	DF	Mean square	F value	*P*-value>F
Model	56.22	9	6.25	34.53	0.01[a]
Linear mixture	0.42	2	0.21	1.16	0.42
X_1X_2	16.67	1	16.67	92.17	>0.00[a]
X_1X_3	27.05	1	27.05	149.51	>0.00[a]
X_2X_3	27.42	1	27.42	151.56	>0.00[a]
$X_1X_2X_3$	2.72	1	2.72	15.02	0.03[a]
$X_1X_2(X_1-X_2)$	0.66	1	0.66	3.67	0.15
$X_1X_3(X_1-X_3)$	0.41	1	0.41	2.24	0.23
$X_2X_3(X_2-X_3)$	0.18	1	0.18	0.99	0.39
Residual	0.54	3	0.18		
Total	56.76	12			

[a]Significant F-values at the 95% confidence level (p-value≤0.05)
DF=Degrees of freedom

APPENDIX B

Regression models of predicted kinetic parameters from analytical method

For first-order kinetics

Activation energy: $142.8X_1+89.3\ X_2+103.3\ X_3-81.9\ X_1\ X_2-105.6\ X_1\ X_3-46.3\ X_2\ X_3+352.43\ X_1\ X_2\ X_3-236.5X_1X_2(X_1\text{-}X_2)-163.2\ X_1X_3(X_1\text{-}X_3)-155.8X_2X_3(X_2\text{-}X_3)$ R^2=0.96 (B.1)

Pre-exponential factor: $(3.7E+12)X_1-(7.9E+09)\ X_2-(7.9E+09)\ X_3-(8.2E+12)\ X_1\ X_2-(8.2E+12)\ X_1\ X_3-(1.0E+11)\ X_2\ X_3+(1.4E+13)\ X_1\ X_2\ X_3-(7.6E+12)\ X_1X_2(X_1\text{-}X_2)-(7.6E+12)\ X_1X_3(X_1\text{-}X_3)-(2.9E+07)\ X_2X_3(X_2\text{-}X_3)$ R^2=>0.99 (B.2)

For n^{th}-order kinetics

Activation energy: $177.3X_1+83.5\ X_2+68.9\ X_3-204.9\ X_1\ X_2-2.7\ X_1\ X_3-23.9\ X_2\ X_3+101.9X_1\ X_2\ X_3-175.4X_1X_2(X_1\text{-}X_2)-65.1\ X_1X_3(X_1\text{-}X_3)+4.7\ X_2X_3(X_2\text{-}X_3)$ R^2=0.96 (B.3)

Pre-exponential factor: $(9.3E+13)X_1-(2.0E+11)X_2-(2.0E+11)X_3-(2.1E+14)X_1X_2-(2.1E+14)X_1X_3-(2.6E+12)X_2X_3+(3.5E+14)X_1X_2X_3-(2.0E+14)X_1X_2(X_1-X_2)-(2.0E+14)X_1X_3(X_1-X_3)+(2.6E+08)X_2X_3(X_2-X_3)$ R^2=>0.99 (B.4)

Reaction order: $1.6X_1+1.1X_2+1.4X_3+18.2X_1X_2+23.2X_1X_3+23.4X_2X_3-47.9X_1X_2X_3-7.0X_1X_2(X_1-X_2)-5.4X_1X_3(X_1-X_3)+3.6X_2X_3(X_2-X_3)$ R^2=0.99 (B.5)

Regression models of predicted kinetic parameters from KAS

For first-order kinetics

Activation energy: $145.3X_1+123.8X_2+200.7X_3+184.8X_1X_2-48.1X_1X_3-88.5X_2X_3-353.5X_1X_2X_3+120.5X_1X_2(X_1-X_2)-85.7X_1X_3(X_1-X_3)+475.5X_2X_3(X_2-X_3)$ R^2=0.97 (B.6)

Pre-exponential factor: $-(4.0E+13)X_1+(6.8E+13)X_2+(2.3E+16)X_3+(2.0E+15)X_1X_2-(4.8E+16)X_1X_3-(5.1E+16)X_2X_3+(9.6E+16)X_1X_2X_3+(5.3E+15)X_1X_2(X_1-X_2)+(5.2E+16)X_1X_3(X_1-X_3)+(5.1E+16)X_2X_3(X_2-X_3)$ R^2=0.99 (B.7)

For n^{th}-order kinetics

Activation energy: $145.3X_1+123.8X_2+200.7X_3+184.8X_1X_2-48.1X_1X_3-88.5X_2X_3-353.5X_1X_2X_3+120.5X_1X_2(X_1-X_2)-85.7X_1X_3(X_1-X_3)+475.5X_2X_3(X_2-X_3)$ R^2=0.97 (B.8)

Pre-exponential factor: $-(3.1E+12)X_1+(5.9E+13)X_2+(2.5E+16)X_3+(1.3E+16)X_1X_2-(5.3E+16)X_1X_3-(5.7E+16)X_2X_3+(7.4E+16)X_1X_2X_3+(2.7E+16)X_1X_2(X_1-X_2)+(5.2E+16)X_1X_3(X_1-X_3)+(6.2E+16)X_2X_3(X_2-X_3)$ R^2=>0.99 (B.9)

Reaction order: $1.4X_1+1.5X_2+1.1X_3+0.8X_1X_2+1.2X_1X_3+0.4X_2X_3+0.1X_1X_2X_3+1.0X_1X_2(X_1-X_2)-2.4X_1X_3(X_1-X_3)-0.1X_2X_3(X_2-X_3)$ R^2=0.79 (B.10)

Regression models of predicted kinetic parameters from OFW

For first-order kinetics

Activation energy: $147.8X_1+126.8X_2+200.8X_3+178.0X_1X_2-67.0X_1X_3-88.1X_2X_3-243.6X_1X_2X_3+135.4X_1X_2(X_1-X_2)-129.8X_1X_3(X_1-X_3)+457.3X_2X_3(X_2-X_3)$ R^2=0.95 (B.11)

Pre-exponential factor: $-(1.1E+13)X_1+(4.2E+13)X_2+(2.4E+16)X_3+(7.9E+15)X_1X_2-(5.1E+16)X_1X_3-(5.5E+16)X_2X_3+(8.5E+16)X_1X_2X_3+(1.6E+16)X_1X_2(X_1-X_2)+(5.1E+16)X_1X_3(X_1-X_3)+(5.5E+16)X_2X_3(X_2-X_3)$ R^2=>0.99 (B.12)

For n^{th}-order kinetics

Activation energy: $147.8X_1+126.8X_2+200.8X_3+178.0X_1X_2-67.0X_1X_3-88.1X_2X_3-243.6X_1X_2X_3+135.4X_1X_2(X_1-X_2)-129.8X_1X_3(X_1-X_3)+457.3X_2X_3(X_2-X_3)$ R^2 = 0.95 (B.13)

Pre-exponential factor: $-(4.2E+12)X_1-(6.3E+13)X_2-(4.3E+13)X_3+(1.5E+16)X_1X_2+(4.1E+15)X_1X_3+(2.2E+15)X_2X_3-(7.5E+16)X_1X_2X_3+(1.9E+16)X_1X_2(X_1-X_2)-(1.7E+16)X_1X_3(X_1-X_3)+(7.2E+15)X_2X_3(X_2-X_3)$ R^2 = 0.94 (B.14)

Reaction order: $1.4X_1+1.5X_2+1.1X_3+0.8X_1X_2+1.2X_1X_3+0.4X_2X_3+0.1X_1X_2X_3+1.0X_1X_2(X_1-X_2)-2.4X_1X_3(X_1-X_3)-0.1X_2X_3(X_2-X_3)$ R^2 = 0.79 (B.15)

APPENDIX C

Contour plots of predicted kinetic parameters from KAS and OFW

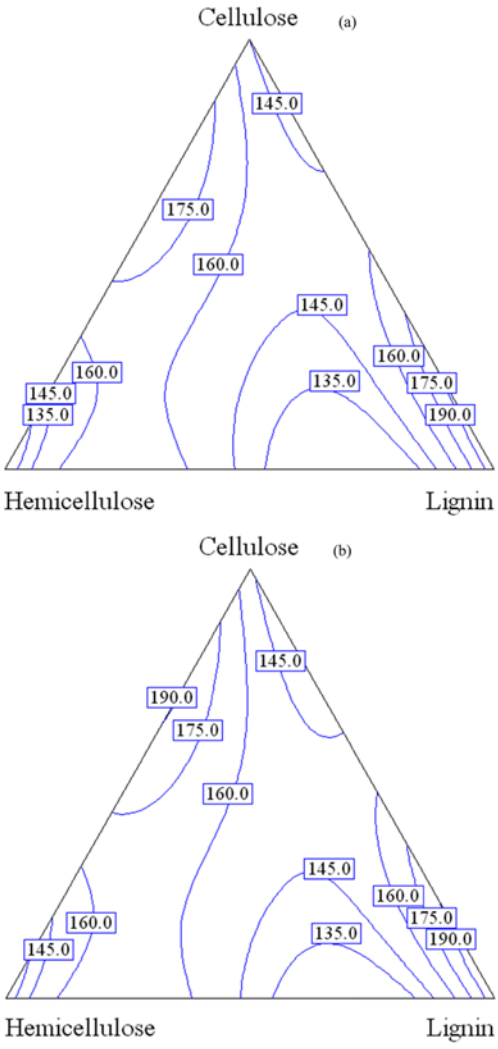

Fig. C.1. Ternary contour plots of predicted activation energy (for first-order kinetics) obtained from KAS (a) and OFW (b).

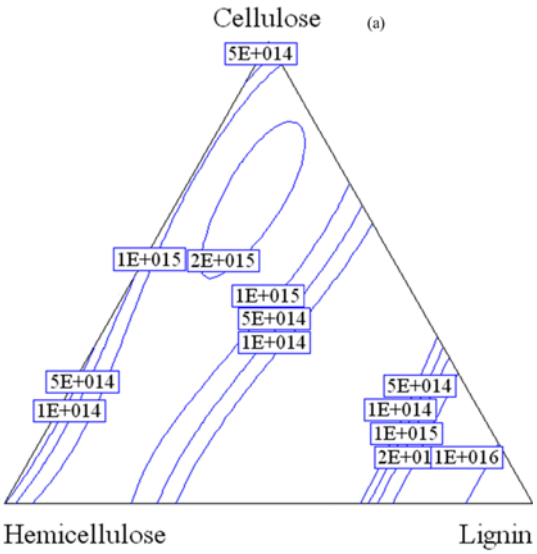

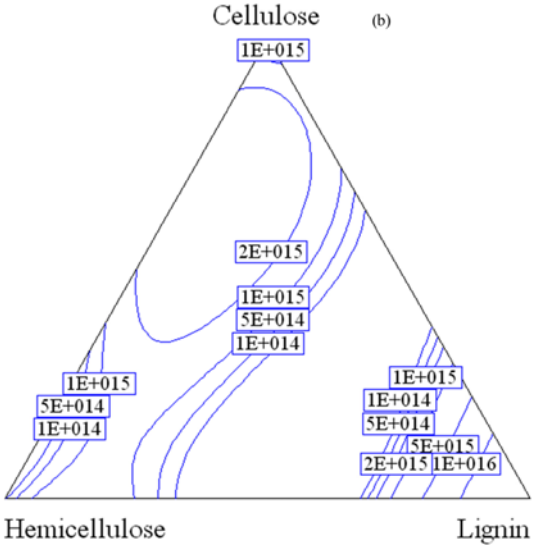

Fig. C.2. Ternary contour plots of predicted frequency factor (for first-order kinetics) obtained from KAS (a) and OFW (b).

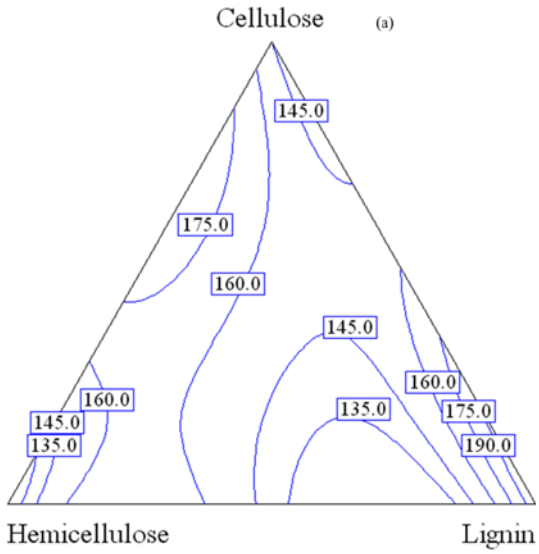

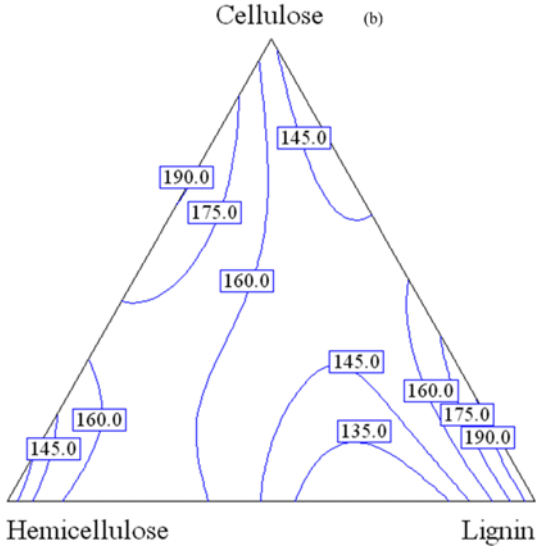

Fig. C.3. Ternary contour plots of predicted activation energy (for any-order kinetics) obtained from KAS (a) and OFW (b).

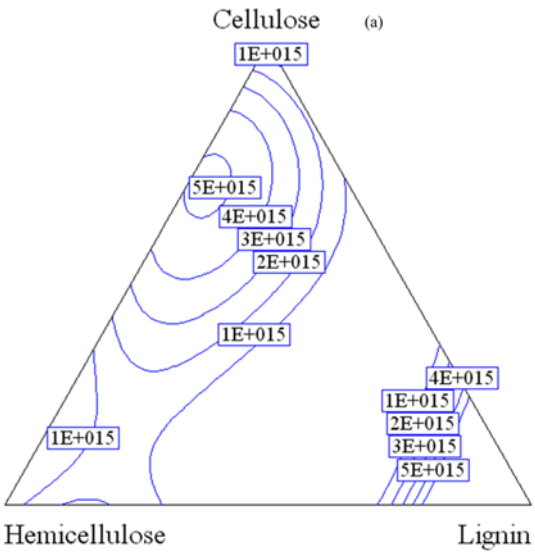

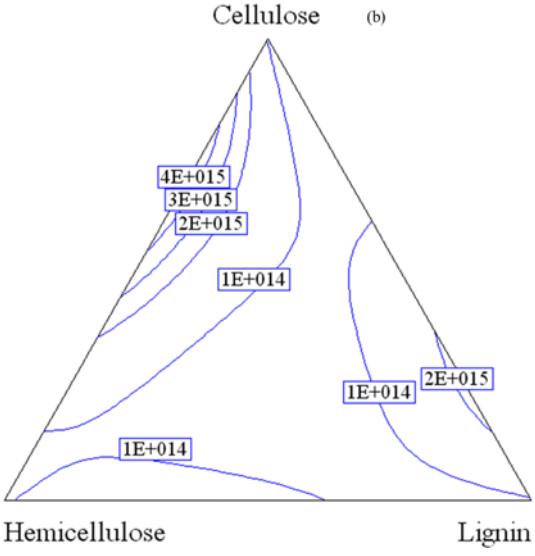

Fig. C.4. Ternary contour plots of predicted frequency factor (for any-order kinetics) obtained from KAS (a) and OFW (b).

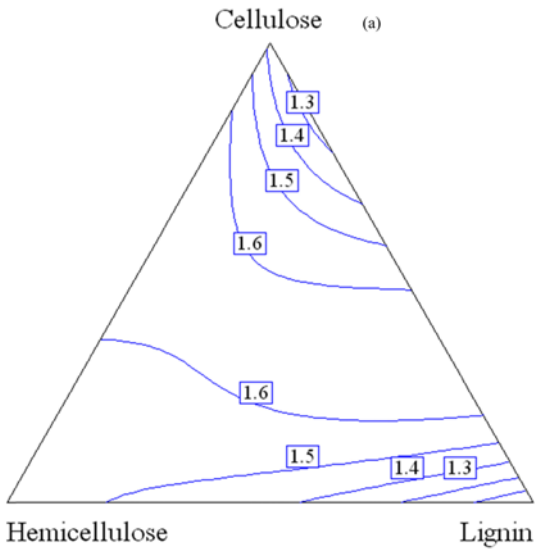

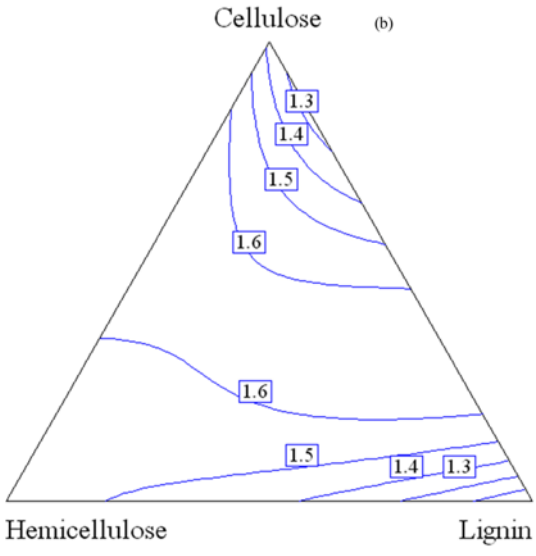

Fig. C.5. Ternary contour plots of predicted reaction order (for any-order kinetics) obtained from KAS (a) and OFW (b).